

# 1 Global Optimization of Multicomponent Distillation 2 Configurations: 2. Enumeration Based Global 3 Minimization Algorithm

AQ4 4 **Rakesh Agrawal**  
5 School of Chemical Engineering, Purdue University, West Lafayette, IN 47907

6 **Ulaganathan Nallasivam, Vishesh H. Shah, Anirudh A. Shenvi, Joshua Huff, and Mohit Tawarmalani**  
7 Krannert School of Management, Purdue University, West Lafayette, IN 47907

8  
9 *DOI 10.1002/aic.15204*  
10 *Published online in Wiley Online Library (wileyonlinelibrary.com)*

11 We present a general Global Minimization Algorithm (GMA) to identify basic or thermally coupled distillation configu-  
12 rations that require the least vapor duty under minimum reflux conditions for separating any ideal or near-ideal multi-  
13 component mixture into a desired number of product streams. In this algorithm, global optimality is guaranteed by  
14 modeling the system using Underwood equations and reformulating the resulting constraints to bilinear inequalities.  
15 The speed of convergence to the globally optimal solution is increased by using appropriate feasibility and optimality  
16 based variable-range reduction techniques and by developing valid inequalities. The GMA can be coupled with already  
17 developed techniques that enumerate basic and thermally coupled distillation configurations, to provide for the first  
18 time, a global optimization based rank-list of distillation configurations. © 2016 American Institute of Chemical Engi-  
19 neers AIChE J, 00: 000–000, 2016

20 **Keywords:** transition split, preferred split, multicomponent distillation, distillation configurations, global optimization

## 24 Introduction

25 Several alternative distillation configurations can be used  
26 for separating an ideal or near-ideal multicomponent mixture  
27 into a desired number of product streams. Many mathematical  
28 models have been proposed for systematically synthesizing all  
29 these possible distillation configurations.<sup>1–5</sup> In these models,  
30 the distillation configurations use the same number of distilla-  
31 tion columns to separate a given feed mixture into the desired  
32 product streams. However, the distillation configurations may  
33 or may not have the same number of heat exchangers. As a  
34 result, these configurations can differ in installation costs.  
35 Moreover, even though they carry out the same separation  
36 task, these configurations have been found to differ signifi-  
37 cantly in their vapor duty requirements, leading to signifi-  
38 cantly different operating costs. It is thus important to identify  
39 a distillation configuration for which the total installation and  
40 operating costs are minimum.

41 Furthermore, distillation configurations for a given sepa-  
42 ration task can even have a different number of distillation col-  
43 umns. A distillation configuration to separate a mixture into  $n$   
44 product streams can be classified as having less than  $(n - 1)$   
45 distillation columns or at least  $(n - 1)$  distillation columns.  
46 The configurations with at least  $(n - 1)$  distillation columns  
47 can be further classified either as basic or non-basic distillation  
48 configurations.<sup>6</sup> Basic configurations have exactly  $(n - 1)$  dis-

49 tillation columns while non-basic distillation configurations  
50 use more than  $(n - 1)$  distillation columns for an  $n$ -component  
51 separation. Configurations with less than  $(n - 1)$  columns are  
52 typically attractive only for limited types of multicomponent  
53 separation problems as pointed out by Shenvi et al.<sup>7</sup>, while  
54 non-basic distillation configurations (that use more than  
55  $(n - 1)$  columns) have been shown, through extensive computa-  
56 tions for four component separations, to have higher operat-  
57 ing costs than optimal basic configurations, as presented by  
58 Giridhar and Agrawal<sup>8</sup>. Non-basic configurations are also  
59 expected to have higher capital costs than basic configurations  
60 due to additional distillation columns and associated heat  
61 exchangers. Therefore, in this work, we only include basic  
62 configurations in our search space.

63 The search space is defined as the set of all possible distilla-  
64 tion configurations that are candidate solutions during the  
65 search for a globally optimal configuration. Structurally, a dis-  
66 tillation configuration can be described by a unique set of dis-  
67 crete binary integer variables. The value of each integer  
68 variable would indicate the presence or absence of the corre-  
69 sponding unit in the configuration. For example, an integer  
70 variable can represent presence or absence of a heat exchanger  
71 at a specific location in a configuration. In addition to this  
72 structural description of a configuration, continuous variables  
73 are also needed to represent internal and external flow rates  
74 and compositions in a configuration. Therefore, each distilla-  
75 tion configuration in a search space is mathematically associ-  
76 ated with a unique set of integer and continuous variables, and  
77 the search for an optimal configuration involves optimization

AQ1

Correspondence concerning this article should be addressed to M. Tawarmalani and R. Agrawal at mtawarma@purdue.edu and agrawalr@purdue.edu.

© 2016 American Institute of Chemical Engineers

78 over both continuous and discrete integer variables. The  
79 search for a globally optimal configuration can be carried out  
80 in two ways. The first approach is to formulate the problem as  
81 a single mixed-integer nonlinear programming (MINLP) prob-  
82 lem<sup>4,5</sup> solved by a local optimization solver. In this approach,  
83 the distillation configuration search space is defined as a math-  
84 ematical superstructure that contains all possible configura-  
85 tions. The MINLP approach attempts to find the globally  
86 optimal solution without enumerating all the configurations  
87 in the search space. As pointed out by Caballero and  
88 Grossmann<sup>4</sup>, this approach faces three important challenges:  
89 unless globality can be assured, (1) in most cases, a feasible  
90 solution is not found because of singularities that arise with  
91 disappearing column sections, (2) Iterations are very time con-  
92 suming, and (3) even if a solution is found, it often corre-  
93 sponds to a poor local optimum.

94 To address these issues, Caballero and Grossmann<sup>4</sup> devel-  
95 oped a super structure based model that could be solved  
96 through a modified version of a logic-based outer approxima-  
97 tion algorithm.<sup>9</sup> In this approach the MINLP problem is  
98 decomposed into an MILP master problem and an nonlinear  
99 programming problem (NLP) sub-problem, with the master  
100 problem being formulated by replacing the nonlinear equa-  
101 tions with their convex outer-approximations. This makes the  
102 master problem less sensitive to column sections that dis-  
103 appear in a particular solution, and also provides a better initial  
104 guess for the NLP sub-problem. The MILP master problem  
105 involves discrete optimization and is solved to generate a fea-  
106 sible configuration. The NLP sub-problem involves continu-  
107 ous optimization and is solved to optimize the feasible  
108 configuration generated by the MILP master problem. This  
109 process is repeated iteratively until the NLP solution starts  
110 worsening relative to a previous iteration. The configuration  
111 associated with current iteration is then selected as the optimal  
112 solution. Observe that this procedure does not guarantee the  
113 global optimality of the solution it identifies.

114 Subsequently, Caballero and Grossmann<sup>5</sup> presented a new  
115 iterative procedure to solve an MINLP problem that includes  
116 thermally coupled configurations in the search space. This  
117 procedure decomposes each problem into a master problem and  
118 sub-problem. In this procedure the integer variables associated  
119 with transfer-stream heat exchangers are assigned values of  
120 zero, that is, they are assumed to be absent during each iteration  
121 of the master problem. This approach thus identifies a  
122 completely thermally coupled (CTC) configuration during  
123 each iteration of the master problem. In the sub-problem, the  
124 heat exchangers are allowed to be present or absent while  
125 freezing the configuration structure to the solution generated  
126 by the master problem. These two steps are repeated iter-  
127 atively until a stopping criterion is met in two consecutive iterations.  
128 This procedure also does not guarantee a globally  
129 optimal solution. The limitation of both these procedures lies  
130 in the decomposition of the original problem into sub-  
131 problems. To guarantee global optimal solution is sought, such a  
132 decomposition cannot be performed.

133 The second approach for identifying an optimal distillation  
134 configuration is to synthesize the complete search space and to  
135 formulate individual NLP problems for each configuration in  
136 the search space. We refer to this approach as an enumeration  
137 based approach. Until now, the optimization of a distillation  
138 configuration was attempted either analytically or by solving a  
139 nonlinear programming problem (which may include integer  
140 variables as well) using state-of-art local optimization solvers.

In the first part of this series of articles, we demonstrated that  
141 the analytical method, referred to as the Sequential Minimiza-  
142 tion Algorithm (SMA), is not a reliable global optimization  
143 tool.<sup>10</sup> Similarly, other researchers such as Giridhar and  
144 Agrawal<sup>1</sup> found that local optimization solvers were often  
145 unsuccessful in finding globally optimal solutions because of  
146 the nonlinear nature of the problem. To overcome this chal-  
147 lenge, they recommended using multiple randomly generated  
148 initial guesses, but still could not guarantee global optimality  
149 while significantly increasing computational burden. Further-  
150 more, in a few cases, no feasible solutions could be found for  
151 some NLP problems by this approach.  
152

In this article, we present a general NLP-based formulation  
153 that can describe all basic and thermally coupled configura-  
154 tions, and can be solved to guaranteed global optimality. We  
155 refer to this formulation as a Global Minimization Algorithm  
156 (GMA), throughout this article. This algorithm is applied to  
157 each basic and thermally coupled distillation configuration to  
158 obtain its corresponding globally minimum vapor duty  
159 requirement. This algorithm uses a bilinear reformulation of  
160 the Underwood equations. To use this algorithm, we first gen-  
161 erate all the configurations in the search space using the  
162 method of Shah and Agrawal<sup>2,3</sup>. Subsequently, GMA-based  
163 optimization of each configuration provides a global optimiza-  
164 tion based rank-list of distillation configurations. GMA is thus  
165 the first algorithm to guarantee that all globally optimal distil-  
166 lation configurations for any ideal or near-ideal multicompo-  
167 nent separation problem will be identified. Unlike the MINLP  
168 approach, this approach does involve the computational effort  
169 of evaluating each individual configuration in the search  
170 space, but is currently the only approach that is able to solve  
171 this problem to global optimality; further, this approach adds  
172 the capability exists to identify all configurations within a pre-  
173 specified percent of the global optimum. A process flow chart  
174 illustrating the key steps of the GMA is shown in Figure 1.  
175 F1 Details about the GMA-based formulation will be described in  
176 the following sections. Strategies for reducing the computa-  
177 tional time will also be discussed.  
178

## Search Space of Distillation Configurations

179 For general multicomponent distillation problems, the  
180 search space is limited to distillation configurations that use  
181 exactly  $n - 1$  distillation columns to separate an ideal or near-  
182 ideal multicomponent mixture into  $n$  product streams. This  
183 search space can be synthesized using the method of Shah and  
184 Agrawal<sup>2,3</sup>, where every feasible distillation configuration for  
185 an  $n$ -component separation is represented as an  $n \times n$  upper  
186 triangular matrix. The upper triangular elements correspond to  
187 streams in a configuration and can take values of either zero or  
188 one. A value of zero indicates that the corresponding stream is  
189 absent in the configuration, while a value of one indicates  
190 presence of the corresponding stream. For example, for a four  
191 component separation, all possible streams that may be present  
192 in a configuration are ABCD, ABC, BCD, AB, BC, CD, A, B,  
193 C, and D (see Figure 2a). The corresponding upper triangular  
194 F2 matrix with possible 0/1 values is shown in Figure 2b. Note  
195 that the main feed stream (element (1,1)) and the final product  
196 streams (elements in the final column) always have values of  
197 one in this matrix. The remaining streams are necessarily  
198 transferred between distillation columns and can take values  
199 of either zero or one. Figure 3 shows a feasible configuration  
200 F3 for a four-component separation. The streams ABC, BCD, and  
201 BC are absent in this particular configuration. The  
202

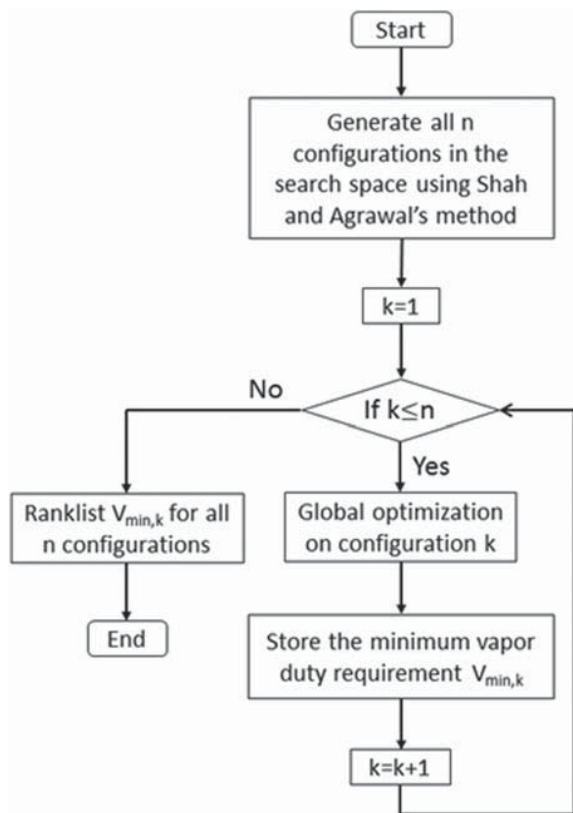


Figure 1. Process flow chart of GMA method.

corresponding stream matrix and 0–1 upper triangular matrix is shown in Figure 4. Any feasible basic distillation configuration is thus represented by a unique 0–1 upper triangular matrix in the matrix method.

Shah and Agrawal<sup>2,3</sup> provide mathematical constraints to ensure that only matrices corresponding to feasible basic distillation configurations are included in the search space. A procedure is also given to convert a feasible 0–1 upper triangular matrix into a distillation configuration as shown in Figures 5a–c. A feasible configuration for a five-component separation is represented by the 0–1 upper triangular matrix shown in Figure 5a. The corresponding stream matrix is shown in Figure 5b. This stream matrix is used to enumerate the splits by starting with the main feed stream followed by each of the transfer streams present in the matrix. For any stream in the matrix, horizontal movement to its right identifies its top product and diagonal movement to its right identifies its bottom product. Therefore, the splits for the matrix shown in Figure 5b are ABCDE to ABC/BCDE, ABC to A/BC, BCDE to BC/CDE, BC to B/C, CDE to CD/E, and CD to C/D. Next each split is assigned to a distillation column, with splits producing the same streams being assigned to the same distillation column. Therefore, split

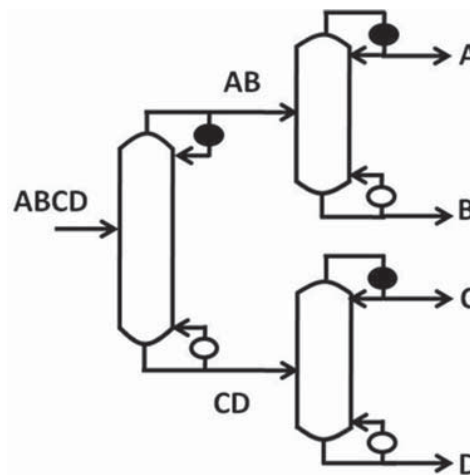


Figure 3. A feasible configuration for a four component separation.

ABCDE → ABC/BCDE is assigned to distillation column 1, splits ABC to A/BC and BCDE to BC/CDE are assigned to distillation column 2 from which the common product stream BC is obtained as a sidestream, split CDE to CD/E is assigned to distillation column 3 and splits BC to B/C and CD to C/D are assigned to distillation column 4 from which the common product stream C is obtained as a sidestream. This information is used to draw the basic distillation configuration shown in Figure 5c. Additional thermally coupled distillation configurations can be derived from a basic configuration by considering all possible instances of the presence or absence of heat exchangers associated with transfer streams. Figure 5d shows a thermally coupled configuration derived from the basic configuration shown in Figure 5c.

To implement the procedure of converting a 0–1 upper triangular matrix to a distillation configuration in a computer program, we assign a numerical identity to each stream. For instance, for a five component separation, Figure 6a shows the convention used by us to assign numerical identities. Therefore, the matrix shown in Figure 5b can be represented mathematically by the matrix shown in Figure 6b. In this article, we refer to this type of matrix as a topology matrix or  $Z_{\text{mat}}$  matrix. A topology matrix corresponds uniquely to each feasible 0/1 matrix and allows easy enumeration of the splits and subsequent assignment to distillation columns in an automated fashion. The main advantage is that the space of 0–1 variables is now significantly smaller than that of super-structure based methods which introduce a binary variable for each type of split possible. For instance, the information summarized in Figure 6c can be obtained from the matrix shown in Figure 6b using a computer program. In Figure 6c, the first column of this matrix is the split number, the second column is the feed to the corresponding split represented by its topology matrix, the third and fourth columns

$\begin{bmatrix} \text{ABCD} & \text{ABC} & \text{AB} & \text{A} \\ 0 & \text{BCD} & \text{BC} & \text{B} \\ 0 & 0 & \text{CD} & \text{C} \\ 0 & 0 & 0 & \text{D} \end{bmatrix}$	$\begin{bmatrix} 1 & 0/1 & 0/1 & 1 \\ 0 & 0/1 & 0/1 & 1 \\ 0 & 0 & 0/1 & 1 \\ 0 & 0 & 0 & 1 \end{bmatrix}$
(a)	(b)

Figure 2. Stream and 0–1 upper triangular matrices for a four component separation.

$\begin{bmatrix} \text{ABCD} & 0 & \text{AB} & \text{A} \\ 0 & 0 & 0 & \text{B} \\ 0 & 0 & \text{CD} & \text{C} \\ 0 & 0 & 0 & \text{D} \end{bmatrix}$	$\begin{bmatrix} 1 & 0 & 1 & 1 \\ 0 & 0 & 0 & 1 \\ 0 & 0 & 1 & 1 \\ 0 & 0 & 0 & 1 \end{bmatrix}$
--	--

Figure 4. Stream and 0–1 upper triangular matrices corresponding to the feasible configuration shown in Figure 2.

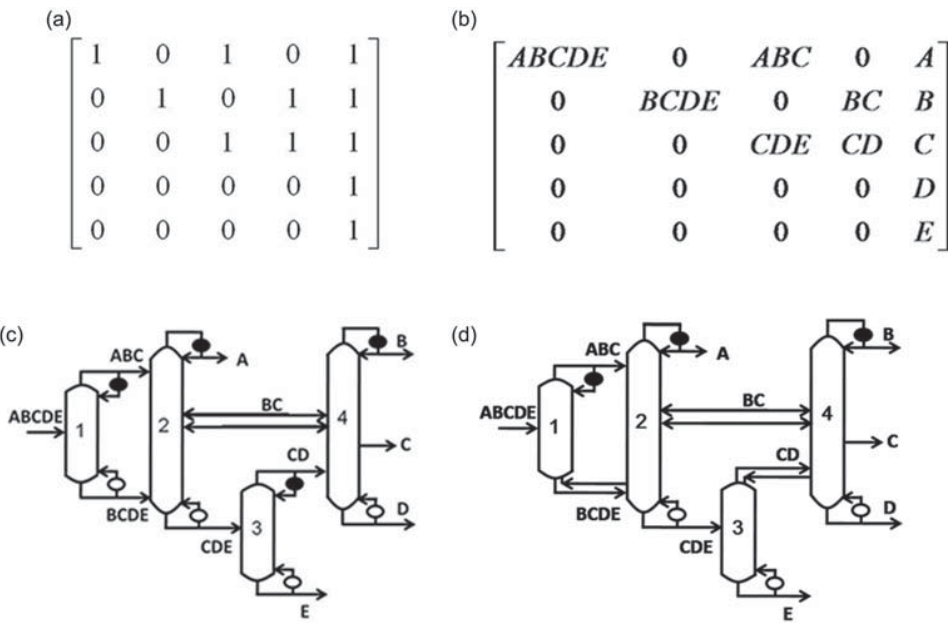


Figure 5. (a) A 0-1 upper triangular matrix corresponding to a feasible distillation configuration for a five component separation. (b) Stream matrix corresponding to the upper triangular matrix shown in Figure 4a. (c) Basic distillation configuration corresponding to the matrix shown in Figures 4a, b. Heat exchangers associated with transfer stream BCDE and CD are replaced by thermal coupling links. (d) One possible thermally coupled configuration derived from the basic configuration shown in Figure 4c.

258 are the top and bottom products of the corresponding split, and  
 259 the fifth column represents the distillation column number to  
 260 which the split is assigned. Because of the information it con-  
 261 tains, this type of matrix is referred to as a connectivity matrix.  
 262 We can thus algorithmically generate a connectivity matrix for  
 263 each feasible 0-1 upper triangular matrix. The connectivity ma-  
 264 trices then allow us to algorithmically formulate an NLP problem  
 265 for each distillation configuration in our search space.

## 266 NLP Formulation

267 Any optimization problem is described by: (1) the decision  
 268 variables, (2) the objective function, and (3) the constraints. In  
 269 the following sections, we present equations for the objective

270 function and the constraints. The parameters, subscripts, vari-  
 271 ables, and variable sets that we have used in writing these equa-  
 272 tions are defined in Appendix A. In all these equations, the  
 273 components are numbered as 1, 2, ..., n in the decreasing  
 274 order of their volatilities. We shall also discuss how these  
 275 equations can be automatically derived using the connectivity  
 276 matrix. In Appendix B, we provide an example detailing the  
 277 equations needed to formulate the nonlinear program for con-  
 278 figuration in Figure 5d.

## 279 Objective Function

280 The objective function is a mathematical expression of the  
 281 desired optimization goal. Since we have only considered

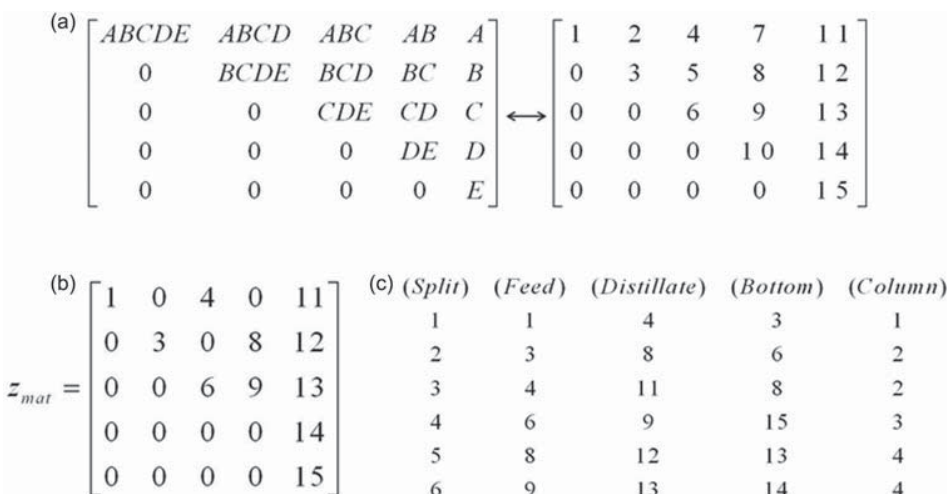


Figure 6. (a) Assigning numerical identities to the streams. (b) Topology matrix or Zmat matrix corresponding to the stream matrix shown in Figure 4b. (c) Connectivity matrix for the distillation configuration corresponding to the feasible configuration represented by 0-1 matrix in Figure 4a.

282 basic and thermally coupled distillation configurations in our  
 283 search space, the capital costs of these configurations are not  
 284 expected to be drastically different from each other. For many  
 285 applications, the operating costs of these configurations can  
 286 differ by significant amounts. Here we assume, as is reasonable,  
 287 that the operating cost of a configuration is proportional to  
 288 the sum of the vapor flows generated at each reboiler of the  
 289 configuration.<sup>11</sup> A more detailed treatment of the relation  
 290 between minimum vapor flow and capital cost will be dis-  
 291 cussed in a later manuscript.

292 The sum of the vapor flows generated at each reboiler in a  
 293 configuration is referred to as the total vapor duty requirement  
 294 of the configuration. The minimum total vapor duty require-  
 295 ment of a configuration is simply the total vapor duty require-  
 296 ment of the configuration calculated under minimum reflux  
 297 conditions. The minimum total vapor duty requirement  
 298 assumes infinite stages, which despite being a theoretical sim-  
 299 plification, produces a reasonable benchmark for comparing  
 300 the operating cost of the configurations. The main advantage  
 301 of this simplification is that it makes the computation more  
 302 tractable. While this approach will not give an exact value of  
 303 actual cost for a configuration, it can be used to rank-list and  
 304 compare different arrangements. Therefore, we use the mini-  
 305 mum vapor duty requirement as the objective function for  
 306 each distillation configuration. A general representation for  
 307 the objective function is:

$$\sum_{s \in \text{COLR}} V_s^{\text{bot}}$$

308 COLR is the set of all the splits which both occur as the bot-  
 309 tom split within a column and have a reboiler at their bottom  
 310 product withdrawal location. The optimization solver is tasked  
 311 with minimizing this objective function. If the assumption of  
 312 minimum reflux is relaxed, the vapor duty requirement of a  
 313 distillation configuration can be estimated by optimizing a rig-  
 314 orous tray-by-tray model. Such a procedure would be equiv-  
 315 alent to optimizing a rigorous ASPEN Plus RADFRAC  
 316 simulation for each configuration and can be relatively time  
 317 consuming. Since the number of feasible configurations in the  
 318 search space is very large, we recommend using the minimum  
 319 reflux assumption since it avoids tray-by-tray computations.  
 320 Our approach thus provides a quick screening tool to do a first  
 321 level screening of the large number of configurations and iden-  
 322 tifies a handful of attractive candidates which can then be stud-  
 323 ied using a computationally intensive tray-by-tray model. We  
 324 use the classical equations derived by Underwood<sup>12</sup> to esti-  
 325 mate the minimum total vapor duty requirement. These equa-  
 326 tions provide a distillation column section based calculation  
 327 method, that is, they do not involve tray-by-tray computations  
 328 of compositions, temperatures, and flows to estimate the vapor  
 329 duty requirement. The equations assume ideal liquid and vapor  
 330 phase behaviors, constant relative volatilities of components,  
 331 and constant and equal latent heats of vaporization for all com-  
 332 ponents in the mixture. These assumptions are thus implicit in  
 333 our model.

### 334 Decision Variables

335 We define the decision variables in a general manner,  
 336 thereby ensuring that they are capable of describing each fea-  
 337 sible distillation configuration in the search space. Conversely,  
 338 the constraints, the objective function and variable sets are

339 uniquely tailored to each distillation configuration based on  
 340 the corresponding connectivity matrix. 340

341 **1. Stream flow rates ( $X_m$ ):** Any distillation column must  
 342 satisfy material balances. To write these constraints we need  
 343 total molar flow rates of each stream. There are  $n \times (n+1)/2$   
 344 upper triangular elements (or streams) in an  $n \times n$  matrix  
 345 corresponding to an  $n$ -component separation. We thus  
 346 declare  $n \times (n+1)/2$  optimization variables for the total  
 347 molar flows of these streams. These variables are represented  
 348 as  $X_m$  in this article, and describe the total molar flow of  
 349 stream  $m$ . For a five component separation, 15  $X_m$  variables,  
 350 one for each stream will be created. 350

351 **2. Component flow rates ( $X_{m,k}$ ):** Underwood's equations  
 352 are solved for each split in the configuration. To estimate the  
 353 vapor duty requirement of a split using Underwood's equa-  
 354 tions, we need the compositions and flow rates of the feed  
 355 stream and the top product stream for each split. If the flow  
 356 rates of each component in these streams are available, then  
 357 the total flow rate of each stream and its composition can be  
 358 calculated. Therefore, we declare the molar flow rate of each  
 359 component in each stream as a decision variable. These vari-  
 360 ables are manipulated by the optimization solver as it tries  
 361 to minimize our objective function. For  $n \times (n+1)/2$  possible  
 362 streams, we thus declare  $n \times (n+1)/2 \times n$  optimization vari-  
 363 ables for the molar flow of each component in each stream.  
 364 These variables are denoted as  $X_{m,k}$ , and describe the flow of  
 365 component  $k$  in each stream  $m$ . For a five component separa-  
 366 tion, 75  $X_{m,k}$  variables, one for each stream-component pair,  
 367 will be created. 367

368 **3. Liquid and vapor flow rates ( $L_m$  and  $V_m$ ):** The thermal  
 369 quality or thermodynamic state of a stream is the fraction  
 370 of the feed flow that is in the liquid phase. To solve Under-  
 371 wood's equations, we need to know the thermal qualities of  
 372 the feed streams of each split in a configuration. Since the  
 373  $n$  final product streams cannot be feed streams to a split,  
 374 we declare  $2 \times [n \times (n+1)/2 - n]$  optimization variables that  
 375 correspond to vapor and liquid flows associated with each  
 376 possible feed stream. For each stream  $m$ , these variables are  
 377 referred to as  $L_m$  and  $V_m$ , respectively. For a five component  
 378 separation, there are a total of ten such stream flows and  
 379 for each feed stream  $L_m$  and  $V_m$  variables are created to  
 380 account for flows in both directions. The thermal quality of  
 381 each stream can be easily calculated from these  $L_m$  and  $V_m$   
 382 variables. In the first part of this series of articles,<sup>10</sup> we  
 383 have defined the thermal quality for various types of  
 384 streams including streams that act as thermal coupling links  
 385 and streams that are side-draws. The same convention is  
 386 used in this article. 386

387 **4. Minimum vapor duty requirements for splits ( $V_s^{\min}$ )**  
 388 and **Underwood roots ( $\theta_{s,r}$ ):** The  $X_{m,k}$ ,  $L_m$ , and  $V_m$  variables  
 389 can be used to formulate Underwood's equations. These  
 390 equations are defined as constraints that relate the minimum  
 391 vapor duty requirement,  $V_s^{\min}$  variables to variables  $X_{m,k}$  and  
 392  $\theta_{s,r}$ . The  $\theta_{s,r}$  variables are referred to in the literature as the  
 393 "Underwood roots." If the feed stream to a split  $s$  has  $p$   
 394 components, the corresponding Underwood's equation has  
 395  $p - 1$  Underwood roots. For each split these are defined as  
 396 decision variables and will be referred to using the symbol  $\theta$   
 397 in this article. 397

398 **5. Actual split vapor flow at top ( $V_s^{\text{top}}$ ) and bottom**  
 399 ( $V_s^{\text{bot}}$ ):  $V_s^{\text{top}}$  and  $V_s^{\text{bot}}$ , respectively, are the vapor flows in  
 400 the rectifying and stripping section associated with split  $s$ .  
 401 We thus require that  $V_s^{\text{top}}$  be no less than  $V_s^{\min}$ , and  $V_s^{\text{top}}$  is 401

402 related to  $V_s^{\text{bot}}$  through a material balance on vapor flow.  
 403 When multiple splits (e.g.,  $s$  and  $s'$ ) are present in the same  
 404 column—where we assume  $s$  is right above  $s'$ —a material  
 405 balance on vapor also links  $V_{s'}^{\text{top}}$  of a lower section with  
 406  $V_s^{\text{bot}}$  of the section immediately above it, and hence  $V_{s'}^{\text{top}}$  is  
 407 related to  $V_s^{\text{top}}$ . Since the vapor flow in the rectifying section  
 408 of one split is related to the vapor flow in the rectifying section  
 409 of another split in the same column, that is, in our  
 410 example, since  $V_s^{\text{top}}$  is related to  $V_{s'}^{\text{top}}$ , the minimum vapor  
 411 flow of a particular split (say  $V_s^{\text{min}}$  for split  $s$ ) can influence  
 412 the vapor flow in every other section of the column containing  
 413 multiple splits. For each split,  $V_s^{\text{top}}$  and  $V_s^{\text{bot}}$  are thus  
 414 defined as decision variables.

415 **6. Split-specific distillate component flow rates ( $\bar{X}_{s,k}$ ):**  
 416 When a stream is produced by two splits, it acts as the bottom  
 417 product for one split and the top product for the other split. In  
 418 such a case, the feed streams of both the splits can contribute  
 419 to the compositions of the common product stream (see  
 420 Appendix C). Therefore, one or more of the component flow  
 421 rates may not be representative of the separation of each split  
 422 and cannot be used directly in Underwood's equations for the  
 423 split. For minimum vapor duty requirement calculations, we  
 424 thus need to estimate the portion of the component flows that  
 425 are contributed only by the split under consideration. These  
 426 component flows are split-specific component flows and we  
 427 need separate variables to represent them. Thus, if there are  $n_s$   
 428 splits in a configuration that separates a feed mixture into  $n$   
 429 product streams, we declare  $n_s \times n$  optimization variables for  
 430 the split-specific distillate component flow rates. For a five  
 431 component separation using the configuration shown in Figure  
 432 5c, the number of splits is 6 and the number of local distillate  
 433 component flow rate variables will be 30.

### 434 Constraints

435 A distillation configuration has to satisfy phase equilibrium  
 436 and mass balance rules. A mathematical expression of these  
 437 rules gives rise to constraints. The following sign convention  
 438 is used for writing these constraints.

439 1. For all splits in a configuration, the order of the splits  
 440 is determined by the  $Z_{\text{mat}}$  number corresponding to their  
 441 feed stream. A split fed by a stream with  $Z_{\text{mat}} = 10$  will  
 442 have a higher split number than a split fed by a stream with  
 443  $Z_{\text{mat}} = 4$ .

444 2. Every flow leaving a lower-numbered split as a product  
 445 is either a pure final product or a feed to a higher-numbered  
 446 split. In either case, a flow is considered positive when leav-  
 447 ing the column containing the lower-numbered split that pro-  
 448 duces it. The net flow of such streams will always be  
 449 positive. Liquid (or vapor) flow variables can be negative;  
 450 that is, they can return to the column in a stream that has a  
 451 net flow leaving the column, given the presence of a larger  
 452 opposing flow of vapor (or liquid), respectively.

453 3. In any molar balance around a particular envelope,  
 454 terms associated with any stream whose net flow is entering  
 455 the envelope are added to the left hand side of the balance;  
 456 terms associated with any stream whose net flow is leaving  
 457 the envelope are subtracted from the left hand side of the  
 458 balance. The right hand side of the balance contains only  
 459 accumulation terms and is always zero.

460 With this convention, we can list the physical rules and  
 461 the type of constraints they give rise to. It will be clear that  
 462 the constraints corresponding to some rules will be different  
 463 for each configuration.

1. **Material balance across columns:** In the absence of 464 chemical reactions, non-condensables, and leaks, the total 465 molar flow entering a distillation column must equal that leav- 466 ing the column. Similarly the total molar flow of any compo- 467 nent entering a distillation column must equal that leaving the 468 column. These rules give rise to the following two types of 469 linear equality constraints 470

$$\sum_{m \in \text{FEEDC}_c} X_m = \sum_{m' \in \text{PRODC}_c} X_{m'} \quad \forall c = 1, \dots, n-1 \quad (1)$$

$$\sum_{m \in \text{FEEDC}_c} X_{m,k} = \sum_{m' \in \text{PRODC}_c} X_{m',k} \quad \forall c = 1, \dots, n-1; \\ \forall k = 1, \dots, n-1 \quad (2)$$

Here the  $\text{FEEDC}_c$  variable set contains all the feed streams 471 entering the distillation column  $c$ , and the  $\text{PRODC}_c$  variable 472 set contains all the product streams leaving distillation column 473  $c$ . The connectivity matrix corresponding to the configuration 474 under consideration contains this information. 475

2. **Total stream flow constraints:** The total flow of any 475 stream is equal to the sum of the flows of each component 476 in the stream, and results in linear equality constraints. 477

$$X_m = \sum_{k=1}^n X_{m,k} \quad \forall m = 1, \dots, n \times (n+1)/2 \quad (3)$$

3. **Feed definition constraints:** The flow rate  $F_k$  of each 479 component  $k$  in the main feed stream  $F$  is specified by the 480 user as a part of the problem definition. These values are 481 assigned to the corresponding decision variables via  $n$  linear 482 equality constraints. One of the requirements for a feed spec- 483 ification is the feed quality  $q_f$ . This must also be defined in 484 an equation. 485

$$X_{1,k} = F_k \quad \forall k = 1, \dots, n \quad (4)$$

$$V_1 = \sum_{k=1}^n F_k (1 - q_f); L_1 = \sum_{k=1}^n F_k (q_f) \quad (5)$$

4. **Constraints for streams that do not exist:** In a given 487 configuration some streams may be absent. For such streams, 488 if we retain the variables in the formulation, we must set the 489 total stream flow and the component flows as 0. This gives 490 rise to two types of linear equality constraints. 491

$$X_m = 0 \quad \forall m \in \text{ABSENTS} \quad (6)$$

$$X_{m,k} = 0 \quad \forall m \in \text{ABSENTS}; \quad \forall k = 1, \dots, n \quad (7)$$

Here, the  $\text{ABSENTS}$  variable set contains all the feed 492 streams that are absent in a given distillation configuration. 493 The connectivity matrix corresponding to the configuration 494 under consideration contains this information. 495

5. **Constraints for definite absence of components in 495 streams:** All the streams except the main feed stream have 496 some components absent. For instance, for a four component 497 separation, the main feed stream is denoted as ABCD since 498 it has some flow of each of the four components. In our 499 model, any other stream such as BC is assumed to have no 500 flow of some components such as A and D. In an actual dis- 501 tillation, all the components will be present in all the 502 streams, in at least trace amounts. However, because of 503 assumption of infinite theoretical stages in our model, 504 streams with trace amounts of components may be treated as 505

506 not containing those components. The variables associated  
507 with the corresponding component flow rates are set to zero:

$$X_{m,k}=0 \quad \forall j=1, \dots, n; \quad \forall i=1, \dots, j; \quad \forall k=1, \dots, i-1 \quad (8)$$

$$X_{m,k}=0 \quad \forall j=1, \dots, n; \quad \forall i=1, \dots, j; \quad \forall k=n+i-j+1, \dots, n \quad (9)$$

508  
509 **6. Net stream flow constraints:** For each stream, the sum  
510 of its liquid and vapor portions must equal its net flow.  
511 Also, the final product streams are liquid-only streams in our  
512 model. Furthermore, transfer streams associated with  
513 condensers are vapor-only streams, while transfer streams asso-  
514 ciated with reboilers are liquid-only streams in our model.  
515 These lead to four types of linear equality constraints.

$$X_m=L_m+V_m \quad \forall m=1, \dots, \frac{n(n+1)}{2} \quad (10)$$

$$\begin{cases} X_m=L_m \\ V_m=0 \end{cases} \quad \forall m=\frac{n(n-1)}{2}+1, \dots, \frac{n(n+1)}{2} \quad (11)$$

$$\begin{cases} X_m=L_m \\ V_m=0 \end{cases} \quad \forall m \in \text{REBOILERS} \quad (12)$$

$$\begin{cases} X_m=V_m \\ L_m=0 \end{cases} \quad \forall m \in \text{CONDENSERS} \quad (13)$$

516 Here, the CONDENSERS and REBOILERS variable set  
517 contains the stream numbers of streams that originate from  
518 condensers or reboilers excluding the final product streams.

519 **7. Distillation constraints:** Based on the  $Z_{\text{mat}}$  matrix dem-  
520 onstrated in Figure 6, it is clear that for any  $(i,j) < n$  the  
521 stream number corresponding to  $Z_{\text{mat}}(i,j)$  is given by  
522  $Z_{\text{mat}}=\binom{j}{2}+i=\frac{j(j-1)}{2}+i$ . Likewise for any stream  $m$  the ROW  
523 and COL variables uniquely identify the values of  $i$  and  $j$   
524 which satisfy  $m=\binom{j}{2}+i$ ;  $n \geq j \geq i$ ; in other words, ROW and  
525 COL read the location of stream  $m$  in the  $Z_{\text{mat}}$  matrix.

526 In non-azeotropic distillation processes, the top product of a  
527 split must get enriched in at least one of the light components  
528 and the bottom product of a split must get enriched in at least  
529 one of the heavy components, relative to the feed stream. For  
530 instance, for the split of ABCD to ABC/BCD, we must ensure  
531 the following inequality constraint in our model.

$$\frac{x_{B,\text{dist}}}{x_{C,\text{dist}}} \geq \frac{x_{B,\text{feed}}}{x_{C,\text{feed}}}, \text{ where } x_{j,\text{stream}} \text{ is the mole fraction of compo-} \\ 532 \text{533} \text{534} \text{535} \text{536} \text{537} \text{538} \text{539} \text{540} \text{541} \text{542} \text{543} \text{544} \text{545} \text{546} \text{547} \text{548} \text{549} \text{550} \text{551} \text{552} \text{553} \text{554} \text{555} \text{556} \text{557} \text{558} \text{559} \text{560} \text{561} \text{562} \text{563} \text{564} \text{565} \text{566} \text{567} \text{568} \text{569} \text{570} \text{571} \text{572} \text{573} \text{574} \text{575} \text{576} \text{577} \text{578} \text{579} \text{580} \text{581} \text{582} \text{583} \text{584} \text{585} \text{586} \text{587} \text{588} \text{589} \text{590} \text{591} \text{592} \text{593} \text{594} \text{595} \text{596} \text{597} \text{598} \text{599}$$

544 A similar constraint is created for each pair of consecutive  
545 overlapping components (where applicable) in the product  
546 streams of each split. Each side of the constraint equation  
547 involves a ratio of component mole fractions belonging to the  
548 same stream. Therefore, these mole fraction terms can be  
549 replaced by the corresponding component flow rate terms. A  
550 rearrangement of terms then converts the constraint to a bilin-  
551 ear inequality constraint.

$$\forall s \in \text{DISTC}$$

$$m=\text{FEEDS}_s; m'=\text{DISTS}_s$$

$$X_{m,k-1} \times X_{m',k} \leq X_{m,k} \times X_{m',k-1}; \quad i=\text{ROW}(m); \quad i'=\text{ROW}(m')$$

$$j=\text{COL}(m); \quad j'=\text{COL}(m')$$

$$\forall k=3, \dots, n-j+i$$

$$(14)$$

These distillation constraints are applicable only when the product streams of a split have at least two overlapping components. The DISTC variable set contains all the splits which meet this criterion, and can be generated in a computer program by using the information in the corresponding connectivity matrix. In Eq. 14,  $i$  and  $j$  represent the row and column number corresponding to the distillate stream under consideration in the  $n \times n$  matrix. The term  $n-j+i$  corresponds to the last component in a stream at the location  $(i, j)$  in the matrix. FEEDS and DISTS give the stream number of the feed and distillate streams. When coupled with the molar balance, Eq. 14 ensures that the bottom stream of a split is also enriched in at least one heavy component.

8. **Thermal coupling constraints:** For streams that serve as thermal coupling links, the vapor portions of their flows must match the vapor flow entering or exiting the appropriate corresponding distillation column. Therefore, for a thermal coupling link connected to the top of a distillation column, the vapor portion of the flow must be set equal to the actual vapor flow above the feed of the top split of the distillation column. Similarly, for a thermal coupling link connected to the bottom of a distillation column, the vapor portion of the flow must be set equal to the actual vapor flow below the feed of the bottom split of the distillation column. These result in two types of linear equality constraints.

$$V_s^{\text{bot}} = -V_m \quad \forall m \in \text{TCBOTT}; \quad c=\text{CVECTOR}(m); \quad s=\text{SBOT}_c \quad (15)$$

$$V_s^{\text{top}} = V_m \quad \forall m \in \text{TCTOP}; \quad c=\text{CVECTOR}(m); \quad s=\text{STOP}_c \quad (16)$$

The TCBOTT variable set contains the stream numbers for the streams which serve as thermally coupled links at the bottom of a distillation column. Similarly the TCTOP variable set contains the stream numbers for the streams which serve as thermally coupled links at the top of a distillation column. The CVECTOR variable set contains information about which distillation column number produces stream  $m$ . SBOT<sub>c</sub> and STOP<sub>c</sub> give the splits that produce (respectively) the bottom and top product of column  $c$ .

9. **Underwood's equations as constraints:** For every split in the configuration, we have to ensure two types of constraints that represent Underwood's equations. The first constraint is referred to as the Underwood feed constraint and is given by Eq. 17. It can be seen that this constraint is an  $(n-j+1)^{\text{th}}$  order polynomial in  $\theta$  (where  $j$  is the column number of the feed stream according to  $Z_{\text{mat}}$ ). Basically, this equation is applied for each feed stream in the distillation configuration and the order of the polynomial in  $\theta$  is the number of components in the corresponding feed stream. For a feed with  $p$  components, the constraint can be written as a  $p^{\text{th}}$  order polynomial in  $\theta$ . Let these roots be  $\theta_1 \geq \dots \geq \theta_p$ . Then, Underwood showed that for  $\alpha_{i+k} \leq \theta_k \leq \alpha_{i+k-1}$  for  $k=1, \dots, p-1$ . The active root is further used to estimate the vapor duty requirement in the second Underwood constraint equation as shown in Eq. 18a. In Eq. 18a,  $V_s^{\text{min}}$  represents the minimum vapor duty requirement in the rectifying section of the split under consideration.

We have observed that it is not necessary to be able to identify this active root of a split ( $\theta_a$ ). We can instead estimate  $V_s^{\text{min}}$  for not just the active Underwood root, but instead for all other Underwood roots as well. The Underwood

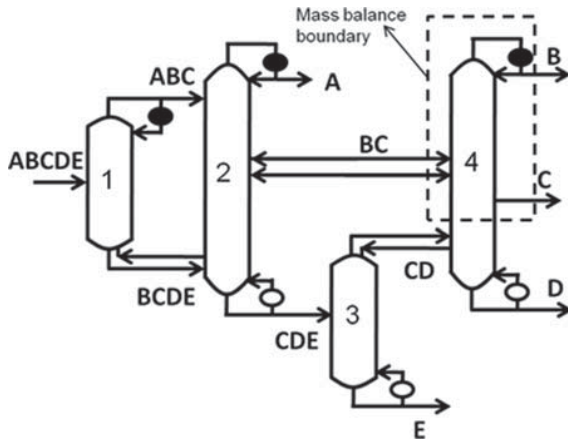


**Figure 7. Example distillate component balance constraint boundary for split CD to C/D.**

root( $s$ ) that results in the largest  $V_s^{\min}$  value has always been observed to be the active root. The largest value of  $V_s^{\min}$  thus corresponds to the minimum vapor duty requirement in the rectifying section of the split under consideration. Therefore, to avoid the difficulty of algorithmically identifying the active root ( $\theta_a$ ) of a split, we use the abovementioned observation and replace the Underwood vapor flow constraint by the equivalent inequality constraint as given by Eq. 18b.

$$\sum_{k=i}^{n-j+i} \frac{\alpha_k X_{m,k}}{\alpha_k - \theta_{s,r}} = V_m \quad \forall s=1, \dots, ns; \quad \forall r=1, \dots, n-j+i; \\ m=\text{FEEDS}_s; \quad i=\text{ROW}(m); \quad j=\text{COL}(m) \quad (17)$$

$$\sum_{k=i}^{n-j+i} \frac{\alpha_k \bar{X}_{s,k}}{\alpha_k - \theta_{s,r}} = V_s^{\min} \quad \forall s=1, \dots, ns; \quad \forall r=1, \dots, n-j+i; \\ i=\text{ROW}(\text{DISTS}_s); \quad j=\text{COL}(\text{DISTS}_s) \quad (18a)$$

$$\sum_{k=i}^{n-j+i} \frac{\alpha_k \bar{X}_{s,k}}{\alpha_k - \theta_{s,r}} \leq V_s^{\min} \quad \forall s=1, \dots, ns; \quad \forall r=1, \dots, n-j+i; \\ i=\text{ROW}(\text{DISTS}_s); \quad j=\text{COL}(\text{DISTS}_s) \quad (18b)$$

In these equations  $i$  corresponds to the first component of the stream under consideration and the term " $n - j + i$ " corresponds to the last component of the stream under consideration. The variables  $\bar{X}_{s,k}$  are split-specific distillate component flow rates.

Two separate cases are encountered in the course of the algorithm. When a split is such that components  $r$  and  $r + 1$  are found in both the top and bottom products of the split, Eq. 18a applies. When  $r$  and  $r + 1$  are not found in both top and bottom product, Eq. 18b will be used. Equation 18b can be thought of as more general; the applicability of Eq. 18a in the previously described cases has been demonstrated in literature.<sup>13</sup>

**10. Split-specific distillate component flow estimation constraints:** These constraints are essentially mass balance calculations across an envelope that covers the top of a distillation column and extends below until it includes the top product of the split under consideration. For example, the envelope for split CD to C/D in the distillation configuration of Figure 5d is shown in Figure 7. The calculations estimate the portions of the component flow rates ( $\bar{X}_{s,k}$ ) in the top product of the split under consideration that originate only

from the feed of the split under consideration. This ensures that we do not include flow contributions from other splits while estimating the vapor duty requirement of the split under consideration using the Eq. 18b.

$$\forall s=1, \dots, ns \\ \bar{X}_{s,k} = \sum_{m \in \text{LPRODA}_s} X_{m,k} - \sum_{m \in \text{FEEDA}_s} X_{m,k} \quad i \in \text{ROW}(\text{DISTS}_s) \\ k=i, \dots, n-j+i \quad j \in \text{COL}(\text{DISTS}_s) \quad (19)$$

$$\forall s=1, \dots, ns \\ \bar{X}_{s,k} \leq X_{m,k} \quad m=\text{DISTS}_s \quad i \in \text{ROW}(\text{DISTS}_s) \quad (20) \\ j \in \text{COL}(\text{DISTS}_s) \\ k=i, \dots, n-j+i$$

$\text{DISTS}_s$  is the distillate product stream of each split  $s$ . The  $\text{LPRODA}_s$  variable set contains the product streams that are above the split  $s$  within the same distillation column and the  $\text{DISTs}_s$  variable set contains all the feed streams above the split  $s$  within the same distillation column.

**11. Vapor balance equations within column:** Once  $V_s^{\min}$  is known for all splits within a column, these minimum vapor requirements must be coupled with a series of vapor balances to determine how much vapor is required at the column reboiler. This is achieved by the following three sets of equations:

$$V_s^{\text{top}} \geq V_s^{\min} \quad \forall s=1, \dots, ns; \quad (21)$$

$$V_s^{\text{top}} = V_s^{\text{bot}} + V_m \quad \forall s=1, \dots, ns; \quad \forall m \in \text{FEEDS}_s; \quad (22)$$

$$V_j^{\text{top}} = V_i^{\text{bot}} + V_m \quad \forall i \in \text{TOP}_c; \forall j \in \text{BOT}_i; \forall m \in \text{SD}_{i,j} \quad (23)$$

Equation 21 dictates that the actual top vapor flow must always exceed the minimum vapor requirement as calculated by Underwood's method. Equation 22 sets the difference between the top and bottom flows of vapor within a split equal to the amount of vapor added or withdrawn by the feed. In Eq. 23,  $\text{TOP}_c$  is a list of all splits in column  $c$  excluding the bottom split, while the  $\text{BOT}_i$  variable set returns the split  $j$  which is immediately below any split  $i$ . This equation enforces the mass balance of vapor at the boundary of two splits using variable set  $\text{SD}_{i,j}$  which is the stream number corresponding to the side draw stream between split  $i$  and split  $j$ .

This completes the description of the objective function and the constraints of our optimization formulation for any given distillation configuration. It can be seen that the objective function is a linear function and all the constraints are linear except Constraints 14, 17, and 18b. The nonlinearity arises in constraint (14) because of the bilinear terms involved in it. The nonlinearity in constraint (17) arises from the fact that it is a polynomial in  $\theta$ . The nonlinearity in constraint (18b) is because it involves fractional terms. Our optimization problem thus has a linear objective function with linear and nonlinear constraints, making it a NLP problem.

For each distillation configuration, a unique NLP problem can be algorithmically generated as described above. The formulation works with any non-azeotropic  $n$ -component

separation problem using  $n - 1$  columns and includes configurations with and without thermal coupling. We automatically generate an NLP problem for each configuration on the fly and solve it to global optimality, with current state-of-the-art solvers. Solving these NLP problems to global optimality is significantly easier than solving a single MINLP problem to global optimality. Our approach then provides a global optimization based rank-list of all possible basic and thermally coupled distillation configurations with respect to their total minimum vapor duty requirements.

### Ensuring Global Optimality

NLP optimization solvers such as GAMS/BARON<sup>14</sup> guarantee global optimality as long as the formulation uses nonlinear functions such as bilinear, fractional, or logarithmic functions and the search space is compact. In our experience, the polynomial inequality (17) can pose a challenge to these solvers. We have therefore reformulated the equation to a more tractable form.

As mentioned before, Underwood showed that all the  $p - 1$  Underwood roots of a  $p^{\text{th}}$  order polynomial lie in between consecutive volatilities of the  $p$  feed components. Mathematically, this results for feed  $m$  with  $i = \text{Row}(m)$ :

$$\alpha_k \geq \theta_{s,k} \geq \alpha_{k+1} \quad (24)$$

GAMS/BARON solver has well defined convex relaxations for standard bilinear/fractional nonlinear functions.<sup>15</sup> These convex relaxations are used in the solver to arrive at the global minimum solution of the NLP through standard branch and bound method<sup>16,17</sup> based global optimization techniques.

One of the disadvantages of using branch and bound techniques is that the convergence can be quite slow. The GAMS/BARON optimization solver overcomes this limitation by using optimality and feasibility based range reduction techniques<sup>18</sup> to speed up the convergence.

### Feasible Initial Guesses

The optimization solver benefits from a feasible and preferably good quality initial guess solution for each configuration's NLP problem. This is particularly true because of the singularity when  $\theta_k$  approaches one of the relative volatilities. We ensure this by obtaining an initial guess using the SMA algorithm that was presented in detail in the first part of this series of articles.<sup>10</sup> The SMA involves analytical calculations only. Therefore, it quickly provides a feasible initial guess solution to the optimization solver. In fact, for some configurations, this solution also turns out to be the optimal solution.<sup>10</sup>

### Improving the Speed of Convergence

The speed of convergence for Branch and Bound based techniques can be improved significantly by providing upper and lower bounds as close as possible to the global optimal solution, for all the optimization variables. In this section, we present some physical insights that can be used to generate good bounds for some key decision variables. For all other decision variables, basic insights from mass and material balance can be used to arrive at the appropriate best bounds.

1. The configuration with highest vapor duty requirement in the search space has to be a sharp split configuration without thermal coupling.<sup>8</sup>

In a sharp split configuration, all splits involved are sharp

splits (i.e., each split does not have any components distributing between its distillate and bottom streams). The sharp split configurations without thermal coupling constitute a very small fraction of search space, and can be solved to global optimality analytically without any optimization iterations.<sup>10</sup> The sharp split configuration without thermal coupling and having the highest vapor duty requirement can thus be easily identified. Let us refer to this vapor duty requirement as Worst of sharp split ( $W_{\text{SS}}$ ) vapor duty. This vapor duty requirement provides an upper bound for the total minimum vapor duty requirement for all the configurations in the search space, and thus provides an upper bound to the objective function in our formulation. It also provides a loose upper bound for the minimum vapor duty requirement for each split of each configuration ( $V_s^{\min}$ ) in the search space.

2. The maximum vapor flow that can occur anywhere in a configuration equals the sum of the  $W_{\text{SS}}$  vapor duty and the vapor flow in the main feed stream.

We know that the upper bound of the minimum vapor duty requirement for any configuration is the  $W_{\text{SS}}$  vapor duty requirement. Since apart from the vapor produced in the reboilers, the only point at which additional vapor can enter a configuration is the main feed point in the first distillation column, the maximum vapor flow that can occur in any section of the configuration is given by the sum of  $W_{\text{SS}}$  and the vapor flow in the feed stream. Let us refer to this vapor flow as  $W_{\text{SS} + F}$ . This vapor flow value can be used as the upper bound for vapor flow in sidedraw streams and thermal coupling links.

3. The configuration with the lowest vapor duty requirement in the search space has to be the fully thermally coupled configuration (FTC).

The FTC is one in which all possible streams of the  $n$ -component separation are present; it has thermal coupling links at all the transfer streams. The global minimum vapor duty for this configuration can be calculated by the SMA method.<sup>10</sup> This configuration has the lowest vapor duty in the search space.<sup>13,19,20</sup> Observe that this configuration may not be practical to operate due to the presence of so many thermal couplings. Regardless, its vapor flow requirement is a mathematical lower bound for the total minimum vapor duty requirement for any configurations in the search space. This also provides a lower bound to the objective function in our formulation.

4. The vapor duty requirement of any split in a distillation configuration is greater or equal to its analytical transition split solution.

While this is true for any split in any configuration, we can exploit this fact only for the first split. This is because the feed to this split is the main feed stream which is completely defined *a priori*. The other splits in the configuration have feeds which may take many different values. The transition split solution for the minimum vapor duty requirement of the first split is easily calculated using the SMA algorithm.<sup>10</sup> This value is used as the lower bound for the corresponding vapor duty variable ( $V_1^{\min}$ ).

5. The Underwood roots can be bounded more tightly using the bounds on corresponding component flows and vapor flows.

From Eq. 17, it can be seen that the Underwood root ( $\theta$ ) depends on the component flows in the feed to the split and the amount of vapor in the feed stream. Also, these roots lie

792 between consecutive relative volatilities of the feed components. 793 However, we can get tighter lower and upper bounds 794 for these roots by analyzing the bounds of the variables in 795 Eq. 17 itself. The term ( $V_m$ ) on the right hand side of Eq. 17 796 represents the vapor flow portion of the feed stream. The following 797 two cases are considered for getting good bounds on 798 this vapor flow.

799 Case 1: The feed stream is associated with a heat 800 exchanger. A stream associated with a reboiler is a saturated 801 liquid (thermal quality = 1) and a stream associated with a 802 condenser is a saturated vapor (thermal quality = 0). This 803 information can be used with the upper and lower bounds of 804 the stream's individual component flows to estimate the 805 upper and lower bounds for the variable,  $V_m$ .

806 Case 2: The feed stream is a thermal coupling link or a 807 sidedraw stream. In this case, the vapor flow can be changed 808 during each optimization iteration. Therefore, we use  $W_{SS+F}$  809 as the upper bound for this vapor flow.

810 Equation 17 relates the vapor flow entering a split with 811 the variables  $X$  and  $\theta_{s,r}$ . Since  $f(X, \theta_{s,r})$ , the function given by 812 the left hand side of Eq. 17, is increasing in  $\theta_{s,r}$ , it follows 813 that the lower bound of the variable  $\theta_{s,r}$  can be calculated by 814 replacing the vapor flow term in Eq. 17 by its lower bound. 815 Similarly, the upper bound of  $\theta_{s,r}$  can be calculated by 816 replacing the vapor flow term in Eq. 17 by its upper bound. 817 For a fixed right hand side value in Eq. 17,  $\theta_{s,r}$  will be lowest 818 when each variable  $X$  is at its the upper bound in terms 819 within the summation which are known to be positive, and 820 at its the lower bound in terms within the summation which 821 are known to be negative. Therefore we get:

$$\sum_{k=i}^r \frac{\alpha_k X_{s,k}^U}{\alpha_k - \theta_{s,r}^L} + \sum_{k=r}^{n-j+i} \frac{\alpha_k X_{s,k}^L}{\alpha_k - \theta_{s,r}^L} = V_s^L \quad (25)$$

822 A similar argument can be used to derive Eq. 28 for the 823 upper bound of  $\theta_{s,r}$ :

$$\sum_{k=i}^r \frac{\alpha_k X_{s,k}^L}{\alpha_k - \theta_{s,r}^U} + \sum_{k=r}^{n-j+i} \frac{\alpha_k X_{s,k}^U}{\alpha_k - \theta_{s,r}^U} \leq V_s^U \quad (26)$$

824 For example, consider a split with feed stream AB, we can 825 find lower and upper bounds of Underwood root  $\theta_1$  that lies 826 between  $\alpha_A$  and  $\alpha_B$  using the bounds of the component flow 827 variables and the vapor flow variables in the Underwood 828 feed equation as shown in Eqs. 27 and 28.

$$\frac{\alpha_A X_{AB,A}^U}{\alpha_A - \theta_1^L} - \frac{\alpha_B X_{AB,B}^L}{\theta_1^L - \alpha_B} = V_{AB}^L \quad (27)$$

$$\frac{\alpha_A X_{AB,A}^L}{\alpha_A - \theta_1^U} - \frac{\alpha_B X_{AB,B}^U}{\theta_1^U - \alpha_B} = V_{AB}^U \quad (28)$$

829 Following this procedure, we obtain tighter bounds of the 830 Underwood roots for all splits in the configuration. This 831 variable bound tightening is important because it avoids the 832 singularities associated with  $\theta_{s,k}$  becoming equal to one of the 833 volatilities.

834 6. The minimum vapor duty of a split can be bounded 835 more tightly using the bounds on the corresponding distillate 836 component flows and Underwood roots.

837 It can be seen that the minimum vapor duty of a split 838 depends on the distillate component flows and the Under- 839 wood roots. Since we already know how to calculate tighter

840 bounds on Underwood roots, we can now get tighter bounds 841 on the minimum vapor duty requirement. For example, for a 842 split  $s$  with feed stream ABC to AB/BC, we can find lower 843 and upper bounds of the minimum vapor flow variable using 844 the bounds of the distillate component flow variables and the 845 bounds on each active Underwood root. Equations 29 and 30 846 give the first set of limiting values on minimum vapor flow 847 if active Underwood root is  $\theta_1$ . In the same way, we can get 848 a second set of limiting values on minimum vapor flow 849 assuming  $\theta_2$  is the active Underwood root. The maximum of 850 these limiting values gives the upper bound and the mini- 851 mum of these limiting values gives the lower bound on the 852 minimum vapor flow requirement for this split. 852

$$\frac{\alpha_A \bar{X}_{s,A}^U}{\alpha_A - \theta_{s,1}^L} - \frac{\alpha_B \bar{X}_{s,B}^L}{\theta_{s,1}^L - \alpha_B} - \frac{\alpha_C \bar{X}_{s,C}^L}{\theta_{s,1}^L - \alpha_C} = V_s^U \quad (29)$$

$$\frac{\alpha_A \bar{X}_{1,A}^L}{\alpha_A - \theta_1^U} - \frac{\alpha_B \bar{X}_{1,B}^U}{\theta_1^U - \alpha_B} - \frac{\alpha_C \bar{X}_{1,C}^U}{\theta_1^U - \alpha_C} = V_s^L \quad (30)$$

## Results

853 To demonstrate the use of our GMA, we apply it to the 854 problem of petroleum crude distillation. Petroleum crude oil is 855 typically separated into the following five fractions: Naphtha 856 (A), Kerosene (B), Diesel (C), Gas Oil (D), and Residue (E). 857 In this article, we consider the heavy crude oil feed parameters 858 that were used by Shah and Agrawal<sup>2</sup>. The relative volatility 859 of each component A, B, C, and D, with respect to E is 860 assumed to be 45.3, 14.4, 4.7, and 2.0, respectively. The feed 861 mixture is assumed to contain 14.4% A, 9.3% B, 10.1% C, 862 3.9% D, and 62.3% E on a molar basis. The feed is a two 863 phase mixture, with the flow corresponding to 90% of the 864 heaviest component (E) being in the liquid phase and the 865 remainder of the flow being in the vapor phase. 866

867 For this five component separation, the method of Shah and 868 Agrawal<sup>2,3</sup> is used to enumerate the complete search space of 869 basic and thermally coupled distillation configurations. We 870 thus obtain 203 basic configurations and 5925 additional con- 871 figurations that range from partial to complete thermal cou- 872 pling, resulting in a total of 6128 candidate configurations. 873 Throughout this section, the configurations are drawn in fully 874 operable arrangements by the method of Agrawal<sup>21,22</sup> these 875 arrangements are completely equivalent in terms of vapor to 876 those such as the configuration drawn in Figure 7. We formu- 877 late the optimization problem in MATLAB and call the 878 GAMS/BARON optimization solver through the GAMS/ 879 MATLAB interface provided by Ferris et al.<sup>23</sup>. 879

880 To demonstrate the need for GMA algorithm, we run the 881 optimization problem in the following three scenarios: 881

### Scenario 1

883 Here, we solve our NLP optimization problem using the 884 NLP solver GAMS/MINOS, without any inputs like feasible 885 initial guesses from our SMA algorithm and without our 886 tighter bounds. An NLP problem is generated and solved for 887 all the 6128 candidate configurations. The following are the 888 key observations from the results of this run. 888

889 1. MINOS could get globally optimal solutions only for 890 2378 candidate configurations out of the search space of 890 6128 configurations. 891

892 2. MINOS concludes that the problem is infeasible for 892 1625 candidate configurations. 893

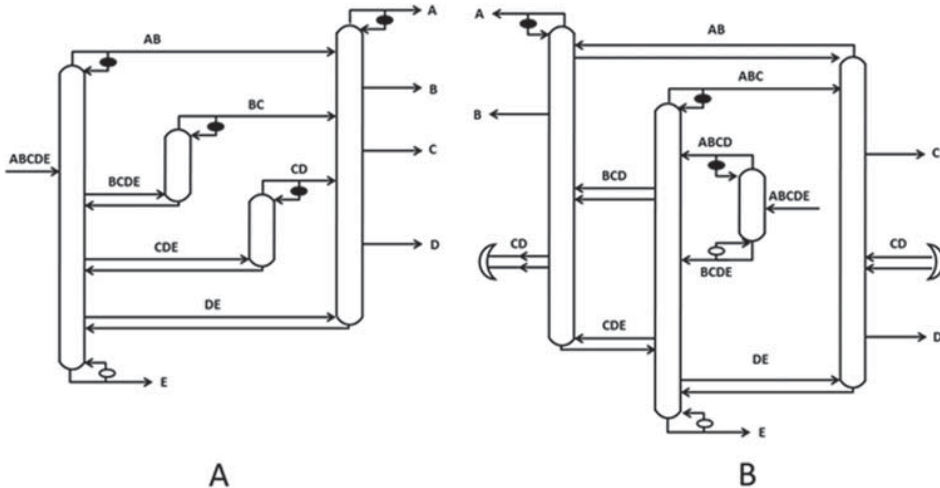


**Figure 8. A/B: Fully operable arrangement of two distillation example configurations for which GAMS/MINOS gets only a locally optimal solution.**

894 3. MINOS gets locally optimal solutions (i.e., those for  
 895 which a superior solution can be identified using GMA) for  
 F8 2125 candidate solutions. Figure 8a shows a configuration  
 896 from this set. For this configuration MINOS gets only an  
 897 intermediate local solution of 1.3678 moles of vapor duty  
 898 requirement per mole of feed flow, which is higher than the  
 899 true optimal solution of 0.7452 moles per mole of feed flow  
 900 for this configuration by 83.5%. Figure 8b shows another  
 901 configuration for which MINOS gets only a locally optimal  
 902 solution of 1.3678 moles of vapor per mole of feed flow,  
 903 which is higher than the globally optimal solution of 0.6996  
 904 moles per mole of feed flow for this configuration by 95.5%.

905 4. Of the 2125 locally optimal solutions, the maximum  
 906 percentage by which the NLP solution is higher than the  
 907 globally optimal solution is 95.5%.

#### 908 **Scenario 2:**

909 Here we solve each of the 6128 NLP optimization problems  
 910 using the NLP solver GAMS/MINOS with initial guesses  
 911 from our SMA algorithm and with tighter bounds on the  
 912 variables.

913 1. MINOS now could obtain the optimal solutions for  
 914 4447 configurations. It terminates infeasible solutions for  
 915 345 configurations and gets only locally optimal solutions  
 916 for 1336 configurations.

917 2. In this run MINOS finds the optimal solution for the  
 918 configuration shown in Figure 8a. For the configuration  
 919 shown (Figure 8b), it gets only a slightly improved inter-  
 920 mediate solution of 1.2224 moles per mole of feed flow, which  
 921 is still higher than the globally optimal solution by 64.3%.  
 922 The reason for this is, that as seen in Figure 8b, this configu-  
 923 ration is a “satellite” configuration with streams transferred  
 924 in opposite directions between two columns. Thus the initial  
 925 guess from the SMA solution is not a very good starting  
 926 point for the optimization solver.

#### 927 **Scenario 3**

928 Here, we solve each of the 6128 NLP optimization problems  
 929 using the global solver GAMS/BARON with initial  
 930 guesses from our SMA method and with tighter bounds on  
 931 variables.

932 1. The global optimization solver could get a locally opti-  
 933 mal solution as good as that in scenario 2 for all 6128 con-

figurations. 5640 of these configurations were solved to  
 935 global optimality that was certifiably within 2% optimality  
 936 tolerance in just 100 s of computational time per configura-  
 937 tion on a Dell Precision T5500. Feasible local optima were  
 938 reached for all remaining configurations and further exami-  
 939 nation revealed the majority of these could also be solved  
 940 globally with additional time.

941 All of the above results clearly demonstrate the importance  
 942 of the GMA method and a global optimization solver like  
 943 BARON to obtain a reliable and guaranteed true rank-list of  
 944 distillation configurations. We have found our GMA algorithm  
 945 to be robust to different feed conditions and different number  
 946 of components; in contrast to local solution methods, all con-  
 947 figurations tested returned feasible answers.

#### 948 **Advantages of the Enumeration Strategy**

949 For the heavy crude oil distillation example, we obtained a  
 950 global optimization based rank-list of all configurations with  
 951 respect to their minimum total vapor duty requirements. The  
 952 lowest vapor duty requirement for this separation is found to  
 953 be 0.6996 moles per mole of feed flow. Since we have access  
 954 to a complete rank-list, we could observe that 175 configura-  
 955 tions have this same minimum vapor duty requirement. There-  
 956 fore, any of these configurations is the globally optimal  
 957 configuration for this separation with respect to our objective  
 958 function of total minimum total vapor duty requirement. 959 These 175 configurations of course include the FTC shown in  
 960 Figure 9. This configuration involves all transfer streams and  
 961 F9 has no transfer stream exchanger. However, several of the  
 962 other configurations have significantly fewer transfer streams  
 963 and significantly fewer thermal coupling links while having  
 964 the same minimum total vapor duty requirement. For instance,  
 965 five such configurations are shown in Figure 10. Therefore,  
 966 F10 having access to a global optimization based rank-list can sig-  
 967 nificantly help process engineers to identify efficient distilla-  
 968 tion configurations that might be more suitable in other  
 969 dimensions which are not easily quantified in a mathematical  
 970 model, such as process safety and controllability.

971 If maximum ease of operability and controllability is known  
 972 to be important, the tools described in this article can be easily  
 973 tailored to produce solutions strong in these aspects with mini-  
 974 mum computing time. For instance, consider another example

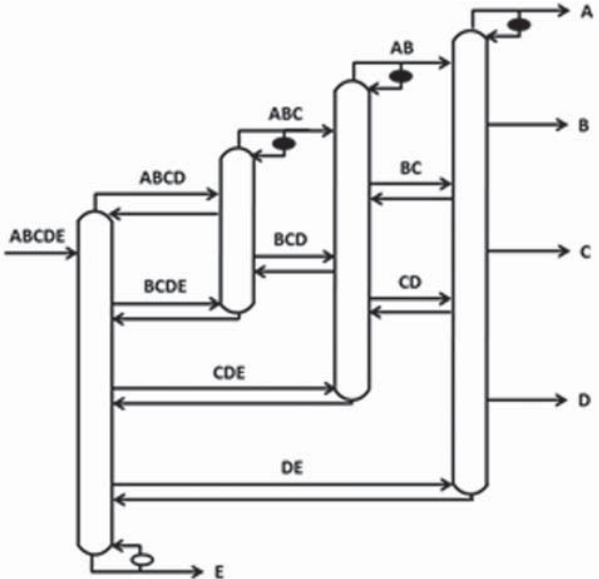


**Figure 9. Fully operable arrangement of fully thermally coupled configuration.**

976 using a general five-component liquid equimolar mixture with  
 977 relative volatilities of components A, B, C, and D with respect  
 978 to E being 39.0625, 15.625, 6.25, and 2.5, respectively. We  
 979 know that the configuration with the minimum total vapor  
 980 requirement will be the FTC, but the fact that this configura-  
 981 tion contains six thermal coupling links can create difficulty in  
 982 constructing and operating it. This ranklist tool can be adapted  
 983 to synthesize alternatives with a vapor requirement within 5%  
 984 of the FTC configuration via the following steps:

1. For a feed flow rate of 100 kmol/h, the minimum total 985 vapor duty requirement of the FTC is 105.156 kmol/h. This 986 value is set as the global lower bound. 987

2. The global upper bound is set as 1.05 times the global 988 lower bound. This will ensure that we only capture those 989 solutions which fall within 5% of the FTC configuration. We 990 avoid solving every possible configuration in our search 991 space to optimality, saving significant computing time. 992

3. The 203 CTC arrangements in the search space are first 993 solved to global optimality. CTC arrangements are those 994 with each transfer stream reboiler and condenser replaced by 995 a thermal coupling link. The FTC configuration is the CTC 996 configuration that contains all possible transfer streams.<sup>24</sup> 997

4. Twenty-six CTC configurations had a vapor require- 998 ment within 5% of the global optimum. For a basic configu- 999 ration, conversion of a condenser or a reboiler to a thermal 1000 coupling link is known to generally lead to a decrease but 1001 never an increase in the overall heat duty of the configura- 1002 tion.<sup>13,19,20</sup> Therefore, for any configuration that does not 1003 belong to the set of 26 CTC configurations, if a thermal cou- 1004 pling were to be replaced with the corresponding reboiler or 1005 the condenser, the overall vapor requirement will never fall 1006 within 5% of the FTC vapor requirement. However, there are 1007 several thermal coupling links within the set of 26 CTC con- 1008 figurations noted above, which when replaced will either not 1009 contribute to an increase in the overall vapor requirement or, 1010 even with the increase, the overall vapor requirement may still 1011 be within 5% of the FTC vapor requirement.<sup>25,26</sup> Thus, for 1012 these 26 configurations, all partially thermally coupled var- 1013 iants with the same topology matrix were optimized using the 1014 same global upper and lower bounds. This approach yielded a 1015 total of 340 configurations with a minimum vapor requirement 1016 within 5% of the globally optimal vapor requirement. Solving 1017

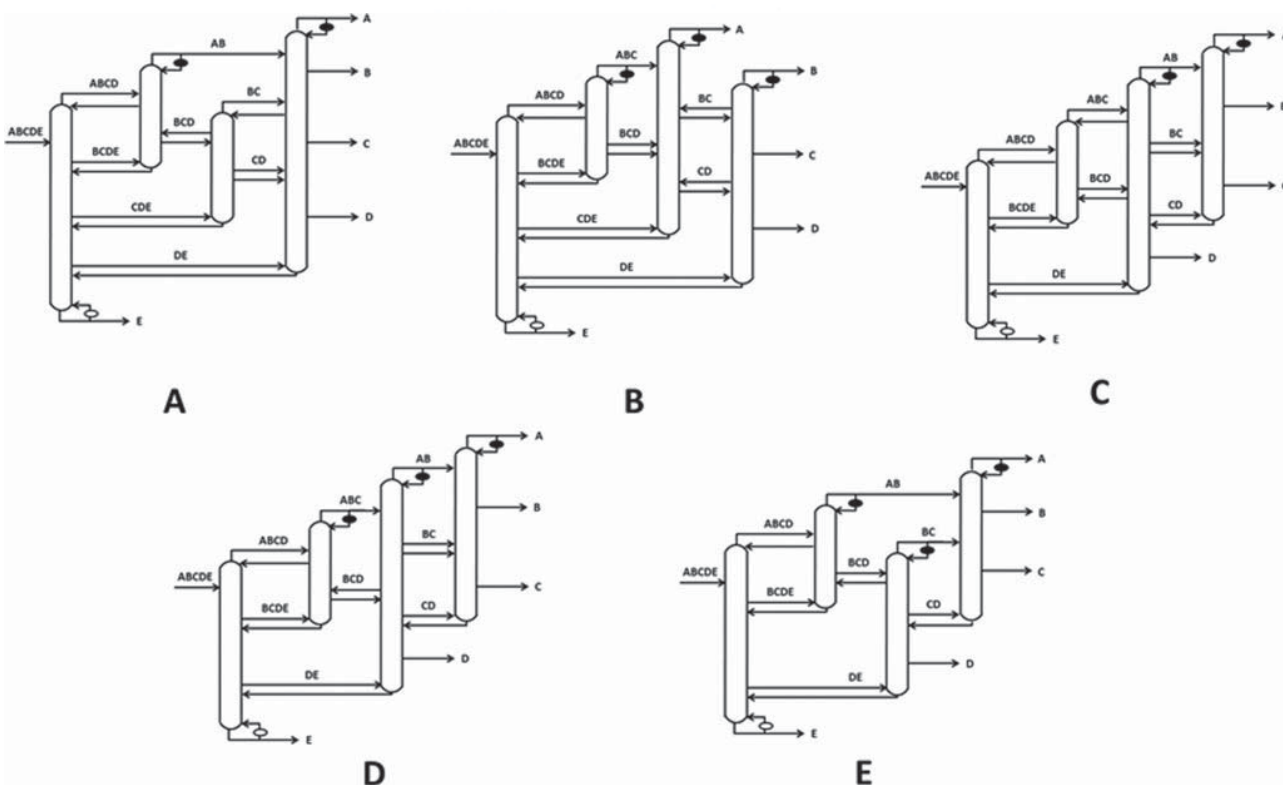


**Figure 10. A/E: Fully operable arrangement of five distillation configurations from the list of the top 175 configura- 985 tions that have the same global minimum total vapor duty requirement.**

1018 only 340 configurations out of 6128 configurations in our  
 1019 search space to global optimality results in a significant reduction  
 1020 in computing time.

1021 After following this method, it was found that for this case  
 1022 338 configurations converged to within 2% optimality tolerance,  
 1023 and the remaining two configurations converged to within 4.6% optimality tolerance within 100 s. Of these 338  
 1024 configurations, 82 have the same vapor requirement as the  
 1025 FTC configuration (105.156 kmol/h), but use fewer thermal  
 1026 couplings. Of these 82 configurations, we can identify ten con-  
 1027 figurations which use only three thermal coupling links (plus  
 1028 one two-way side draw stream), compared to the six thermally  
 1029 coupled links (plus three sidedraw streams) used by the FTC  
 1030 configuration. One of these configurations is pictured in Figure  
**F11** 11. There also exist multiple configurations with only two  
 1031 thermally coupled links (plus one two-way sidedraw stream),  
 1032 which are within 5% of the globally optimal vapor duty. Figure  
**F12** 12 shows one such configuration with two thermal cou-  
 1033 pling links, which has a minimum vapor duty requirement of  
 1034 107.948 kmol/h. This has 2.7% more vapor duty than the  
 1035 global minimum. Thus a practicing engineer can evaluate the  
 1036 trade-off between energy savings and reduced complexity  
 1037 from the point of easy operation and stability and make an  
 1038 informed decision that best suits the design needs of the  
 1039 application.

1040 This example illustrates how the use of a ranklist with the  
 1041 GMA method and BARON solver helps identify the right con-  
 1042 figuration by considering the design and operability in tandem  
 1043 with the energy efficiency of the system in a reasonable com-  
 1044 puting time. We have also developed a visual tool that sim-  
 1045 plifies such a selection process. The tool allows quick selection  
 1046 of a subset of configurations by specifying constraints such as  
 1047 heat duty range of interest, number of acceptable thermal cou-  
 1048 pling links, and presence or absence of specific splits. By spec-  
 1049 ifying such filters, one can quickly and visually observe  
 1050 flowsheets fulfilling these requirements. This allows an engi-  
 1051 neer to narrow the choice from thousands of available config-  
 1052 urations to a select few on the fly.

1053 In some situations, there may be significant uncertainty in  
 1054 the composition and flow rate of the feed mixture. In such a

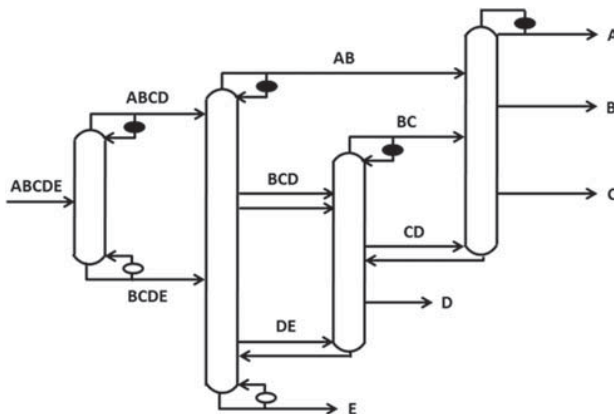


**Figure 12.** Fully operable arrangement—available five-component configuration with 1.027 times minimum vapor duty and two thermally coupled links

1055 situation, one can generate global optimization based rank-  
 1056 lists for some representative feed conditions, and then identify  
 1057 a configuration that is close to optimal for many of these dif-  
 1058 ferent feed conditions.

## Conclusions

1059 Previous work has demonstrated the need for a GMA due to  
 1060 the lack of optimality guarantee from sequential methods.<sup>10</sup> We have presented a general GMA that utilizes a reformulation of Underwood's equation to obtain a global optimization based rank-list of basic and thermally coupled configurations. We have used the minimum total vapor duty requirement as the objective function in our analysis. Our approach provides for the first time, a global optimization framework to identify optimal and near-optimal distillation configurations for ideal or near-ideal multicomponent separations. Our results demonstrate the limitations of using local optimization based NLP solvers. We also presented strategies based on fundamental and physical insights to improve the robustness and the speed of convergence of the distillation sequencing algorithm. Our approach relies on the enumeration of all the configurations in the search space, and allows practicing engineers to select optimal or near-optimal configurations while also taking into account difficult-to-quantify aspects such as control, operability, safety, and feed fluctuations.

1061 Our general framework can be easily tailored to include capital cost and utility costs for specific distillation applications. We shall detail such enhancements in a subsequent paper.

## Acknowledgments

1062 The authors thank the US Dept. of Energy, award DE-FG36-06GO16104 for providing financial support for this work. The authors also thank Zheyu Jiang for his work on improving convergence and robustness of the optimization program.

## Literature Cited

1. Giridhar AV, Agrawal R. Synthesis of distillation configurations: II. A search formulation for basic configurations. *Comp Chem Eng*. 2010;34:84–95.
2. Shah VH, Agrawal R. A matrix method for multicomponent distillation sequences. *AICHE J*. 2010;56(7):1759–1775.

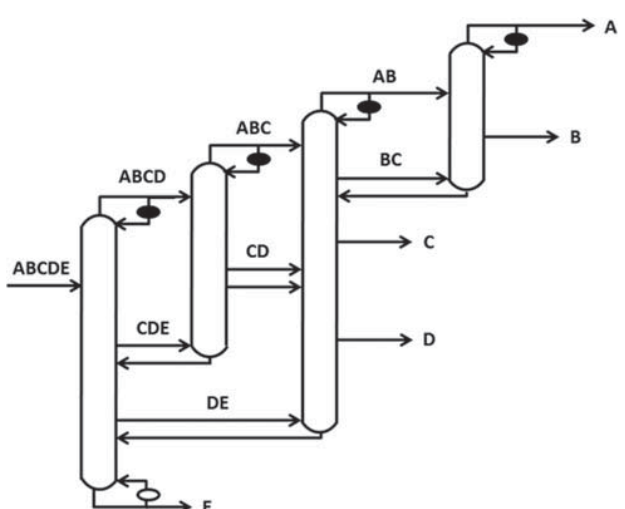


**Figure 11.** Fully operable arrangement—a five-component configuration with globally minimum vapor duty and only three thermally coupled links.

1098 3. Shah VH, Agrawal R. Conceptual design of zeotropic distillation  
1099 processes. In: Gorak A, Sorensen E, editors. *Distillation: Fundamentals and Principles*, Ch. 7. Academic Press, 2014: 271–303.

1100 4. Caballero JA, Grossmann IE. Generalized disjunctive programming  
1101 model for optimal synthesis of thermally linked distillation columns.  
1102 *Ind Eng Chem Res*. 2001;40:2260–2274.

1103 5. Caballero JA, Grossmann IE. Design of distillation sequences: from  
1104 conventional to fully thermally coupled distillation systems. *Comp Chem Eng*.  
1105 2004;28:2307–2329.

1106 6. Agrawal R. Synthesis of multicomponent distillation configurations.  
1107 *AICHE J*. 2003;49:379–401.

1108 7. Shenvi AA, Shah VH, Zeller JA, Agrawal R. A synthesis method  
1109 for multicomponent distillation sequences with fewer columns.  
1110 *AICHE J*. 2012;58(8):2479–2494.

1111 8. Giridhar AV, Agrawal R. Synthesis of distillation configurations: I.  
1112 Characteristics of good search space. *Comp Chem Eng*. 2010;34:73–  
1113 83.

1114 9. Turkay M, Grossmann IE. A logic based outer approximation algo-  
1115 rithm for MINLP optimization of process flowsheets. *Comp Chem Eng*.  
1116 1996;20:959.

1117 10. Nallasivam U, Shah VH, Shenvi AA, Tawarmalani M, Agrawal R.  
1118 Global optimization of multicomponent distillation configurations: I.  
1119 Need for a reliable global optimization algorithm. *AICHE J*. 2013;  
1120 59(3):971–981.

1121 11. Rod V, Marek J. Separation sequences in multicomponent rectifica-  
1122 tion. *Coll Czech Chem Commun*. 1958;24:3240.

1123 12. Underwood AJV. Fractional distillation of multicomponent mixtures.  
1124 *Chem Eng Prog*. 1948;44(8):603–614.

1125 13. Fidkowski ZT, Agrawal R. Multicomponent thermally coupled sys-  
1126 tems of distillation columns at minimum reflux. *AICHE J*. 2001;47:  
1127 2713–2724.

1128 14. Tawarmalani M, Sahinidis NV. The branch-and-reduce optimization  
1129 navigator (BARON), GAMS solver for global optimization of non-  
1130 linear (NLP) and mixed-integer nonlinear programs (MINLP), 2005.

1131 15. Tawarmalani M, Sahinidis NV. *Convexification and Global Optimiza-  
1132 tion in Continuous and Mixed-Integer Nonlinear Programming*.  
1133 Kluwer Academic Publishers, 2002.

1134 16. Edgar TF, Himmelblau DM, Lasdon LS. *Optimization of Chemical  
1135 Processes*. McGraw-Hill Chemical Engineering Series, McGraw-Hill  
1136 Book Company, 2001.

1137 17. Horst R, Tuy H. *Global Optimization: Deterministic Approaches*.  
1138 Springer, 1996.

1139 18. Sahinidis NV. Global optimization and constraint satisfaction: the  
1140 branch-and-reduce approach. COCOS 2002, LNCS 2003;2861:1–16.

1141 19. Fidkowski ZT, Krolkowski L. Thermally coupled system of distilla-  
1142 tion columns: optimization procedure. *AICHE J*. 1986;32:537–546.

1143 20. Halvorsen IJ and Skogested S. Minimum energy consumption in  
1144 multicomponent distillation. 3. More than three products and gener-  
1145 alized Petlyuk arrangements. *Ind Eng Chem Res*. 2003;42:605–615.

1146 21. Agrawal R, Fidkowski ZT. More operable arrangements of fully  
1147 thermally coupled distillation columns. *AICHE J*. 1998;44(11):2565–  
1148 2568.

1149 22. Agrawal R. A method to draw fully thermally coupled distillation  
1150 column configurations for multicomponent distillation. *Chem Eng  
1151 Res Des*. 2000;78(3):454–464.

1152 23. Ferris MC, Jain R, Dirkse S. GDXMRW: interfacing GAMS and  
1153 MATLAB. <http://research.cs.wisc.edu/math-prog/matlab.html>, 2011.

1154 24. Agrawal R. Synthesis of distillation column configurations for a mul-  
1155 ticomponent separation. *Ind Eng Chem Res*. 1996;35:1059–1071.

1156 25. Agrawal, R. Thermally coupled distillation with reduced number of  
1157 intercolumn vapor transfers. *AICHE J*. 2000;46:2198–2210.

1158 26. Shah, VH, Agrawal, R. Are all thermal coupling links between mul-  
1159 ticomponent distillation columns useful from an energy perspective?  
1160 *Ind Eng Chem Res*. 2011;50:1770–1777.

## 1162 Appendix A

1163 In this section, we define the input parameters, subscripts,  
1164 variables and variable sets that have been used in the  
1165 formulation.

### 1166 Input Parameters

1167  $q_f$  = thermal quality (or liquid fraction) in the main feed stream  
1168  $F_k$  = molar flow rate of component  $k$  in the main feed stream  
1169  $n$  = number of components in the main feed stream

$\alpha_k Z$  = relative volatility of component  $k$  with respect to the heaviest  
1170 component

### 1171 Subscripts Used in the Model Definition

$c$  = distillation column number: 1, ...,  $n - 1$   
1172  $i$  = row number in  $n \times n$  matrix: 1, ...,  $n$   
1173  $j$  = column number in  $n \times n$  matrix: 1, ...,  $n$   
1174  $k$  = component number: 1, ...,  $n$   
1175  $ns$  = number of splits in a given configuration  
1176  $m$  = stream number: 1, ...,  $n \times (n+1)/2$   
1177  $r$  = underwood root number  
1178  $s$  = split number

### 1179 Variables

$L_m$  = liquid portion of the flow of stream  $m$   
1180  $X_m$  = total flow of a stream  $m$   
1181  $X_{m,k}$  = flow of component  $k$  in stream  $m$   
1182  $X_{s,k}$  = flow of distillate component  $k$  contributed by split  $s$   
1183  $V_m$  = vapor portion of the flow of stream  $m$   
1184  $V_{bo}^s$  = actual vapor flow below the feed of split  $s$   
1185  $V_s^{\min}$  = minimum vapor duty requirement for the split  $s$   
1186  $V_s^{\top}$  = actual vapor flow above the feed of split  $s$   
1187  $\theta_a$  = active Underwood root for a split  
1188  $\theta_{s,r}$  = underwood root  $r$  of the split  $s$

### 1189 Variable Sets

Note: The examples given here for each variable set corre-  
1190 sponds to the distillation configuration in Figure 5d.

1191 ABSENTS {Streams that are absent in the configuration}

1192 e.g., {2, 5, 7, 10}

1193 BOT<sub>s</sub> {Split located directly below split  $s$  in a column}

1194 e.g., {6} for  $s = 5$

1195 BOTT<sub>s</sub> {Bottom product stream of a split  $s$ }

1196 e.g., {6} for  $s = 2$

1197 COL {Matrix column locations of streams}

1198 e.g., {1, 2, 2, 3, 3, 4, 4, 4, 5, 5, 5, 5, 5}

1199 COLR {Split numbers which are the bottom split in their  
1200 respective column AND contain a reboiler at their bottom  
1201 product}

1202 e.g., {1, 2, 4, 6}

1203 CONDENSERS {Streams associated with condensers except  
1204 the final product streams}

1205 e.g., {4}

1206 CVECT {Distillation column number that produces the given  
1207 stream}

1208 e.g., {0, 0, 1, 1, 0, 2, 0, 2, 3, 0, 2, 4, 4, 4, 3}

1209 DISTC {Splits for which distillation constraints are  
1210 applicable}

1211 e.g., {1}

1212 DIST<sub>s</sub> {Distillate product stream of a split  $s$ }

1213 e.g., {8} for  $s = 2$

1214 FEEDA<sub>s</sub> {Feed streams above split  $s$  within the same column}

1215 e.g., {8} for  $s = 6$

1216 FEEDC<sub>c</sub> {Feed streams entering the distillation column  $c$ }

1217 e.g., {3, 4} for  $c = 2$

1218 FEEDS<sub>s</sub> {Feed stream of a split  $s$ }

1219 e.g., {3} for  $s = 2$

1220 LPRODA<sub>s</sub> {Product streams above split  $s$  within the same  
1221 column including the split's top product}

1222 e.g., {11, 8} for  $s = 2$

1223 PRODC<sub>c</sub> {Product streams exiting the column  $c$ }

1224 e.g., {6, 8, 11} for  $c = 2$

1225 REBOILERS {Streams associated with reboilers except the  
1226 final product streams}

1227 e.g., {6}

1228 ROW {Matrix row locations of streams}

1229 e.g., {1, 1, 2, 1, 2, 3, 1, 2, 3, 4, 1, 2, 3, 4, 5}

1284 STOP<sub>c</sub> {Split that produces thermally coupled top product of  
1285 column  $c$ }  
1286 e.g., {4} for  $c = 3$   
1287 SBOT<sub>c</sub> {Split that produces thermally coupled bottom product  
1288 of column  $c$ }  
1289 e.g., {1} for  $c = 1$   
1290 SD<sub>i,j</sub> {Stream number of the side draw stream between split  $i$   
1291 and split  $j$ }  
1292 e.g., {8} for  $i = 3$  &  $j = 2$   
1293 TCBOTT {Thermal coupling links replacing reboilers in the  
1294 configuration}  
1295 e.g., {3}  
1296 TCTOP {Thermal coupling links replacing condensers in the  
1297 configuration}  
1298 e.g., {9}  
1299 TOP<sub>c</sub> {List of splits in column  $c$ , excluding the bottom split  
1300 in  $c$ }  
1301 e.g., {5} for  $c = 4$

## 1302 Appendix B

1303 We provide the objective function equation and all the con-  
1304 straint equations for the configuration shown in Figure 5d.

### 1305 Objective Function

$$1306 \min (V_2^{\text{bot}} + V_4^{\text{bot}} + V_6^{\text{bot}})$$

### 1307 Constraints

#### 1309 1. Material balance across columns

1310 Molar flow balance for distillation column 1:

$$1311 X_1 = X_3 + X_4 \quad (B1)$$

1311 The component molar flow balance for component 1 for col-  
1312 umn 1:

$$1313 X_{1,1} = X_{3,1} + X_{4,1} \quad (B2)$$

1313 Where  $X_1$  represents molar flow of stream ABCDE and  $X_{1,1}$   
1314 represents the molar flow of component A in the stream  
1315 ABCDE and so on.

#### 1316 2. Total stream flow constraints

1317 For the stream ABC:

$$1318 X_4 = X_{4,1} + X_{4,2} + X_{4,3} \quad (B3)$$

#### 1318 3. Feed definition constraints

1319 For component 1:

$$1320 X_{1,1} = F_1 \quad (B4)$$

$$1321 V_1 = (1 - q_F) \sum_{j=1}^5 F_j; L_1 = (q_F) \sum_{j=1}^5 F_j \quad (B5)$$

#### 1320 4. Constraints for streams that do not exist

$$1321 X_m = 0 \quad \forall m \in \{2, 5, 7, 10\} \quad (B6)$$

$$1321 X_{m,k} = 0 \quad \forall m \in \{2, 5, 7, 10\}; \forall k = 1, \dots, 5 \quad (B7)$$

### 5. Constraints for definite absence of components in streams

1322 Constraints for stream 8, that is, stream BC:

$$1323 X_{8,k} = 0; k = 1 \quad (B8)$$

$$1324 X_{8,k} = 0; k = 4, 5 \quad (B9)$$

### 6. Net stream flow constraints

1325 For feed stream 8, product stream 11, reboiler stream 6 and  
1326 condenser stream 4:

$$1327 X_8 = L_8 + V_8 \quad (B10)$$

$$1328 X_{11} = L_{11}; V_{11} = 0 \quad (B11)$$

$$1329 X_6 = L_6; V_6 = 0 \quad (B12)$$

$$1330 X_4 = V_4; L_4 = 0 \quad (B13)$$

### 7. Distillation constraints

1328 For overlapping component B and C in split 1 (ABCDE to  
1329 ABC/BCDE):

$$1330 X_{1,2} \times X_{4,3} \leq X_{1,3} \times X_{4,2} \quad (B14)$$

### 8. Thermal coupling constraints

1331 For stream BCDE and stream CD:

$$1332 V_1^{\text{bot}} = -V_3 \quad (B15)$$

$$1333 V_3^{\text{top}} = V_9 \quad (B16)$$

### 9. Underwood's equation as constraints

1333 For split 2 (BCDE to BC/CDE):

$$1334 \frac{\alpha_2 X_{3,2}}{\alpha_2 - \theta_{2,r}} + \frac{\alpha_3 X_{3,3}}{\alpha_3 - \theta_{2,r}} + \frac{\alpha_4 X_{3,4}}{\alpha_4 - \theta_{2,r}} + \frac{\alpha_5 X_{3,5}}{\alpha_5 - \theta_{2,r}} = V_3 \quad \forall r = 1, 2, 3 \quad (B17)$$

$$1335 \frac{\alpha_2 \bar{X}_{2,2}}{\alpha_2 - \theta_{2,r}} + \frac{\alpha_3 \bar{X}_{2,3}}{\alpha_3 - \theta_{2,r}} \leq V_2^{\text{min}} \quad \forall r = 1, 2, 3 \quad (B18)$$

### 10. Local distillate component flow estimation constraints

1335 For split 2 (BCDE to BC/CDE), for component B:

$$1336 \bar{X}_{2,2} = X_{11,2} + X_{8,2} - X_{4,2} \quad (B19)$$

$$1337 \bar{X}_{2,2} \leq X_{8,2} \quad (B20)$$

### 11. Vapor flow balance throughout column

1337 For column 2:

$$1338 V_2^{\text{top}} \geq V_2^{\text{min}}; V_3^{\text{top}} \geq V_3^{\text{min}} \quad (B21)$$

$$1339 V_2^{\text{top}} = V_2^{\text{bot}} + V_3; V_3^{\text{top}} = V_3^{\text{bot}} + V_4 \quad (B22)$$

$$1340 V_3^{\text{bot}} = V_2^{\text{top}} - V_8; \quad (B23)$$

## Appendix C

1339 All calculations in this manuscript are performed under the  
1340 following assumption:

1342 When multiple splits share a column, the minimum vapor  
1343 flow for each split can be found by solving the Underwood feed  
1344 and distillate equations corresponding to each split, and then  
1345 assuming a "mixing section" connecting the two splits; out of this  
1346 mixing section a single stream is drawn with a composition calcu-  
1347 lated by completely mixing the products calculated individually  
1348 for each split. The total vapor flow required by the column is  
1349 equal to the greater of the two individual vapor flow requirements.  
1350 This arrangement is assumed to be identical to a system that uses

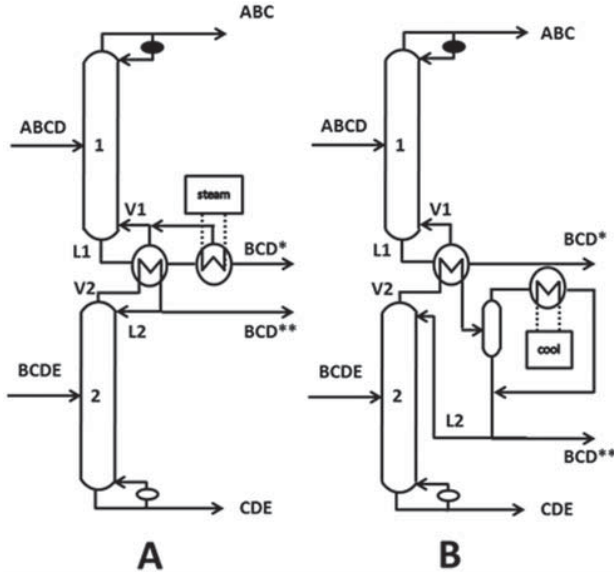


**Figure 13. A/B: Possible heat exchange options for operating both splits using [amount of vapor =  $\max(V_1, V_2)$ ]. A: If  $V_1 > V_2$ , using heat from  $V_2$  to create part of  $V_1$  leads to a total of only  $V_1$  vapor requirement from utility. B/C: If  $V_2 > V_1$ , all of  $V_1$  can be generated by heat exchange with  $V_2$ ; the remainder of  $V_2$  is condensed using either cool utility or the liquid stream of a nearby thermal coupling.**

heat integration to arrive at the same total vapor requirement for performing two separate splits, followed by mixing.

Assume two quaternary splits, S1 and S2, in a system with five components; each is treated separately. Each split produces

a product we call BCD; however, when allowed to assume their minimum vapor flows, the compositions of the two BCD streams may differ (we will refer to them generally as compositions BCD\* and BCD\*\*).

Figure 13 shows some possible example heat integration arrangements (which assume constant latent heat) that would allow operation of both splits independently at their own vapor duty requirements using only the larger of the two individual vapor requirements as the total vapor requirement. In the case where  $V_1$  (the top split's vapor flow) is higher than  $V_2$  (the bottom split's vapor flow), the heat from the first column can provide part of the second column's duty through heat exchange, resulting in a total vapor requirement from utility of only  $V_1$  rather than  $V_1 + V_2$  (Figure 13a).

If  $V_2 > V_1$  and the condensation done in the column is associated with cold utility, Figure 13b demonstrates an arrangement which uses part of the heat available in  $V_2$  to vaporize  $V_1$ , and uses cold utility only for the condensation of  $V_2$ . Once again, this requires only a total of  $V_2$  to be generated by hot utility, rather than  $V_1 + V_2$ . Thus, it has been demonstrated that there are many arrangements capable of operating two splits at a vapor duty of only  $\max(V_1, V_2)$ . In choosing instead to use the arrangement of directly transferring vapor within the column to operate at a vapor duty of  $\max(V_1, V_2)$  we can be sure that the vapor duty could be duplicated through some form of heat exchange. Throughout this article, we assume that an arrangement such as Figure 13 could be designed for any two splits sharing the same column to achieve the vapor duty achieved by taking the maximum of the two. Due to this assumption, we do not optimize configurations by considering these different heat transfer arrangements. Instead, our model uses the simpler calculation of treating the maximum vapor requirement of all stacked splits (adjusted for feed and product streams as described in the Constraints section) as the column's vapor requirement.

Manuscript received Nov. 29, 2015, and revision received Feb. 5, 2016.

AQ1: Please check whether the author affiliations and corresponding details are OK as typeset.

AQ2: Please provide publisher location for Refs. 3, 15, 16, and 17.

AQ3: Please provide complete publication details for Ref. 14.

AQ4: Please confirm that given names (red) and surnames/family names (green) have been identified correctly.

**WILEY**  
**Author Proof**